fibers

MDPI

Article

Mechanical Performances of Natural Textiles for Eco-Friendly Composite Materials: A Comparative Assessment

Gianfranco Stipo [1,*], Valerio Alecci [1], Mario De Stefano [1], Stefano Galassi [1], Maria Cristina Salvatici [2] and Maria Luisa Satta [1]

[1] Department of Architecture, University of Florence, Piazza F. Brunelleschi 6, 50121 Florence, Italy; valerio.alecci@unifi.it (V.A.); mario.destefano@unifi.it (M.D.S.); stefano.galassi@unifi.it (S.G.); marialuisa.satta@unifi.it (M.L.S.)

[2] Institute of Chemistry of OrganoMetallic Compounds, ICCOM-CNR Via Madonna del Piano 10, 50019 Florence, Italy; salvatici@ceme.fi.cnr.it

* Correspondence: gianfranco.stipo@unifi.it

Highlights

What are the main findings?

- The mechanical properties of ten different natural textiles were compared after an all-natural protective treatment referred to as "hornification" process.
- Hornification-induced changes in the fiber morphology were found by using a Scanning Electron Microscope (SEM).

What are the implications of the main findings?

- After 1 to 5 hornification cycles, some fibers like banana, henequen, coir and sisal increased their strength.
- The results of this study represent a promising starting point for future evaluations regarding the integration of natural fibers in innovative and fully sustainable composite materials.

Abstract

In the last decades, composite materials made of synthetic fibers embedded in organic or inorganic matrices have been successfully used for strengthening reinforced-concrete and masonry buildings. The scientific community is currently discussing the low sustainability of these materials and their environmental impact due to the production process, the life cycle, and the generation of potentially harmful waste. In this context, the use of natural textiles represents a promising solution, alternative to conventional synthetic fibers, aimed at designing an innovative composite material obtained from renewable resources with no energy consumption and greatly reducing the impact of building activities on the environment. In this paper, an experimental assessment of ten different natural textiles is presented in order to compare their mechanical properties for possible use in innovative, eco-friendly composite materials. Mechanical tensile tests were performed on the ten different textiles before and after an all-natural protective treatment referred to as the "hornification" process. Treatment-induced changes in the fiber morphology were also analyzed using a scanning electron microscope (SEM), which provided high-resolution images of the surface and cross-sectional area of the fibers. Considering that the current demand for sustainable building materials capable of ensuring a greener future for the construction industry is on the rise, the promising results obtained in this study could be useful to the academic community and building industry.

check for updates

Academic Editor: Damien Soulat

Received: 25 August 2025
Revised: 16 October 2025
Accepted: 29 October 2025
Published: 4 November 2025

Citation: Stipo, G.; Alecci, V.; De Stefano, M.; Galassi, S.; Salvatici, M.C.; Satta, M.L. Mechanical Performances of Natural Textiles for Eco-Friendly Composite Materials: A Comparative Assessment. *Fibers* **2025**, *13*, 148. https://doi.org/10.3390/fib13110148

Keywords: eco-friendly composites; natural fibers; mechanical assessment; hornification; SEM analysis

1. Introduction

In recent decades, composite materials have been successfully used for the structural retrofitting of existing buildings. FRPs (Fiber-Reinforced Polymers) represented a first valid alternative to well-known techniques traditionally based on metal devices or reinforced-concrete insertions [1]. FRPs have shown great effectiveness at strengthening both reinforced-concrete [2] and masonry [3–5] structures, thanks to the high-strength carbon fibers embedded in a polymeric matrix. However, FRPs also highlight some drawbacks, such as the low compatibility with traditional materials, the sensitivity to high temperatures, and the reduced breathability, which compromise their suitability for the restoration of historic buildings [6].

Therefore, to overcome these critical issues, the first thought was to replace the epoxy resin with an inorganic matrix, and new composite materials, called TRMs (Textile-Reinforced Matrices), were conceived. TRMs consist of high-strength fabric—such as glass, carbon, basalt, or PBO (Polybenzoxazole)—embedded in an inorganic lime-based mortar matrix (FRLM, Fiber-Reinforced Lime Matrix) or cement-based mortar matrix (FRCM, Fiber-Reinforced Cementitious Matrix). Compared to FRPs, TRM composites provide greater compatibility with historic substrates, offering less invasive and more suitable solutions for the conservation of the masonry building heritage. Numerous studies available in the scientific literature confirm the effectiveness of TRMs in the strengthening of masonry members, including vaults [7], arches both at the intrados [8] and extrados [9], columns [10,11], and panels [12,13].

TRMs ensure a good bond performance because the sliding basically occurs at the fiber–matrix interface and the historic masonry substrate is preserved from the peeling phenomenon [14]. Several experimental results concerning the bond property of TRM composites obtained by different test setups are available in the literature [15–18].

However, despite the abovementioned advantages, TRMs also have some critical environmental issues related to the use of synthetic or mineral fibers, of which production, disposal, and end-of-life management are characterized by high-energy consumption. In this context, current innovative research is therefore moving towards the use of more sustainable components, with the aim of reducing the environmental impact of composite materials without compromising their structural performance.

Today there is a growing interest in the use of TRM composites assembled with natural fibers as an alternative to synthetic ones. As is known, natural fibers can be divided into three main categories based on their origin: animal, vegetable, and mineral [19]. Plant-based fibers are completely green, and, in fact, they are derived from renewable resources with a sustainable life cycle, as they are able to absorb more CO_2 than they emit during their production. This makes them particularly attractive in terms of reducing the ecological footprint of building materials.

Recently, the use of natural plant-derived fibers for composite materials has attracted growing interest in both commercial and academic circles for its positive effect in the field of environmental sustainability and energy efficiency [20]. However, although successfully used in structural reinforcement, the scientific investigations are rather limited. Only a few results are available [21], and they are basically focused on fibers of hemp [22], flax [23], jute [24], and sisal [25].

Furthermore, the few comparative analyses available in the literature [26,27] show conflicting data. A comparison between the mechanical performances of different fibers appears to be a complex challenge. The first problem is associated with the assemblage of natural fibers into composite materials due to their hydrophilic capacity, i.e., their tendency to absorb water and, as a result, increase in volume. This behavior is due to the presence of hydroxyl groups (-OH) in cellulose, hemicelluloses, and lignin, i.e., the main constituents of natural fibers. These functional groups establish a strong net of hydrogen bonds between the different macro-molecules [28,29] and, when natural fibers are exposed to moisture, water interferes with these internal bonds, causing new hydrogen bonds between hydroxyl groups and water molecules. This process induces significant swelling of the fibers and shrinkage during the drying or curing process and, in the case of natural fibers embedded in a lime or cement mortar matrix, it generates a progressive loss of adhesion between the fiber and the mortar matrix. In this case, the formation of cracks and reductions in mechanical properties and durability can be expected [25,30,31].

Hydrophilicity is a significant challenge for the use of plant fibers in composite materials. Some investigations available in the literature have analyzed and compared the effectiveness of different strategies to optimize the integration of natural fibers into composite materials. The common and diffused approach involves the application of surface coatings to create a protective membrane in order to reduce moisture absorption and preserve the integrity of the fibers over time.

The coatings of jute and sisal fibers with styrene-butadiene rubber (XSBR) show an improvement in tensile strength [32], while the use of waterborne polyurethane (WPU) [33] and polyurethane enriched with graphene nanoparticles [34] shows a general improvement in the mechanical properties of natural fibers. Another study, conducted by Menna et al. [35], analyzed the influence of epoxy-impregnated hemp textiles in FRCM composites, highlighting a significant increase in their mechanical performances.

The application of polymer-based coatings to protect natural fibers improves their tensile strength and fiber-to-matrix adhesion (due to the reduced water absorption) while compromising the main environmental benefits of using natural fibers, i.e., their biodegradability, renewability, and zero-energy consumption.

In order to favor low-impact and environmentally friendly solutions, it is possible to adopt a specific treatment known as the “hornification” process. The hornification process is a physical treatment applied to lignocellulosic fibers, consisting of repeated drying and rewetting cycles, aimed at modifying their internal structure and improving the mechanical stability and structural performance [36,37]. During these cycles, the removal and subsequent reabsorption of water induce irreversible structural rearrangements within the cellulose microfibrils, leading to reductions in porosity and lumen size. These microstructural modifications result in a lower water absorption capacity, an increase in stiffness, and, in some cases, an improvement in tensile strength, depending on the chemical composition of the fiber and its lignin content.

In some cases, hornification can be combined with chemical treatments to enhance its effectiveness. Treatments with chemical agents, such as those used in alkalinization processes or solvent washing, compromise the mechanical properties and adhesion of natural fibers to composite materials. As a result, the ecological characteristics of the final composite material are severely reduced, affecting the environmental impact of the production process and generating potentially harmful waste and residues. For this reason, among the available treatment techniques, the hornification process emerges as the most promising, allowing for a significant increase in the mechanical performance and durability of the natural textile without resorting to harsh chemicals.

In this study, the mechanical properties of the main natural fibers available on the world market were compared. Tensile tests were carried out on untreated fibers and, after the hornification process, tests were repeated to assess the effect of such a process on the mechanical properties of the fibers. Treatment-induced changes in the fiber morphology were qualitatively analyzed using a scanning electron microscope (SEM), which provided interesting insights into the effectiveness of the applied treatments [38].

In detail, the SEM provided high-resolution images of the surface and cross section of the fibers, allowing the following structural and morphological changes to be observed: roughness, fractures, and deformations.

The experimental data allowed for the identification of the type of fiber with the best mechanical properties before and after the hornification process. The final results and considerations could be useful for both engineering practice and future academic research referring to the design of fully sustainable and compatible composite materials.

This paper is organized as follows: In Section 2 the natural fibers analyzed are listed and described as a function of their components, origin, and size; Section 3 describes the experimental program; finally, Sections 4 and 5 are dedicated to the discussion of the results and the conclusions, respectively.

2. Materials and Methods

Natural vegetal fibers are composed of fibrous bundles whose main components are cellulose, hemicellulose, lignin, and pectin. These components determine the mechanical, physical, and chemical properties of the fibers. Pectin acts as a binder for the elementary micro-fibers that comprise the fibrous bundle. Elementary fibers are mainly composed of cellulose, organized into microfibrils with a highly crystalline and ordered structure. Hemicellulose, characterized by a less regular structure, is woven between the cellulose microfibrils, creating a three-dimensional network that restricts their movements. Lignin is a hydrophobic polymer deposited in the interfibrillar spaces and provides rigidity to the structure [39,40].

In more detail, the mechanical strength of fibers depends essentially on the cellulose content. The presence of cellulose ensures high strength, while an excess of lignin content compromises flexibility and makes the fibers more brittle [41,42]. In addition, a key parameter is the fibrillar angle, that is, the inclination of the microfibrils with respect to the longitudinal axis (Figure 1) of the fiber: the smaller the angle, the higher the tensile strength [37,43].

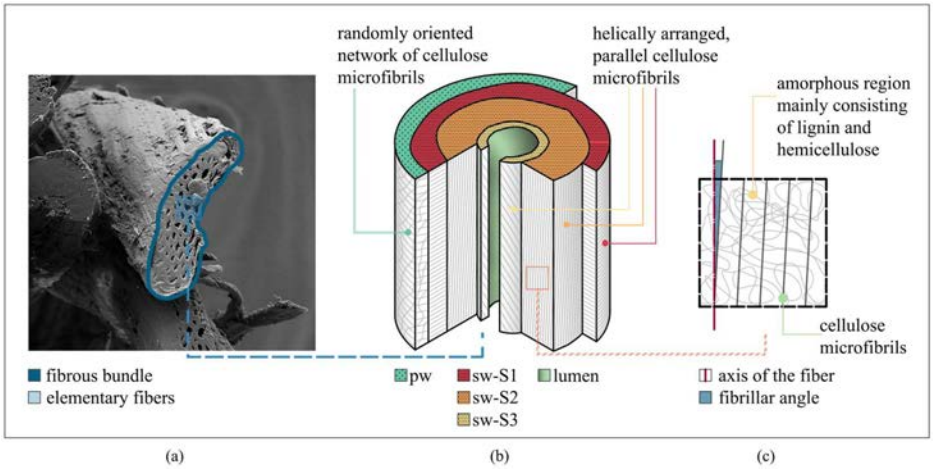

Figure 1. (**a**) SEM image of the cross section of a sisal fiber (scale bar = 1 mm), (**b**) structure of the elemental fibers (pw: primary wall; sw: secondary wall), and (**c**) the relationship between the fiber axis and the cellulose microfibrils (microfibril angle).

In this study, ten types of natural fibers—among the most widespread on the market—were analyzed and mechanically tested. All the fibers were achieved in the form of rolls and specimens hand-assembled in the laboratory. Their main components and the corresponding content percentages as available in the literature are reported in Table 1 [37,44–48].

Table 1. Compositions of the tested natural fibers.

Fibers	Cellulose (%)	Hemicellulose (%)	Lignin (%)	Microfibrillar/Spiral Angle (Degree)
Banana	64	20	5	-
Hemp	70–74.4	17.9–22.4	3.7–6	6.2
Coir	31–42	10–20	40–46	-
Cotton	82.7–95	2–5.7	0.7–1.6	-
Henequen	75–77	4–8	13–14	-
Jute	61–74.4	13.6–20.4	12–13	8.0
Flax	70–73	18–20.6	2–2.2	10.0
Ramie	68–76.2	13–16.7	0.6–1	7.5
Raffia	53	13	24	-
Sisal	60.5–78	10–25.7	8.0–12.1	20

The fibers analyzed in this study have different origins. Within the set of fruit fibers, coconut fiber was selected and examined in detail. It is obtained from the fibrous husk that surrounds the fruit of the plant. Cotton is a fiber obtained from the protective coating of the seeds through ginning and cleaning processes.

Flax, hemp, and jute are stem fibers extracted through a retting process which allows for the separation of the fibers from the woody components. Other stem fibers considered in this research include banana and ramie fibers.

Among the leaf fibers, sisal and henequen were analyzed. Their processing involves mechanical decortication, aimed at separating the fibers from the vegetal pulp of the leaves. Finally, among the leaf fibers, raffia was also tested.

Table 2 reports the types of plants, geographic origins, diameters, weights, and densities of the ten fiber typologies tested in the experimental campaign. The density was calculated through the following formula:

$$\rho = \frac{A}{A - B} \cdot \rho_w \quad (1)$$

where A is the mass in air (g); B is the mass in liquid (g); and ρ_w is the density of the immersion liquid (g/cm^3).

Table 2. Properties of the natural fibers under investigation. The value of the standard variation is in italics, and the coefficient of variation is in parenthesis.

Fibers	Plants	Origin	Diameter (mm)	Weight (g/m)	Density (g/cm^3)
Banana	*Musa textilis*	India	1 *0.09* (0.092)	0.67 *0.31* (0.467)	1.35 *0.13* (0.096)
Hemp	*Cannabis sativa*	Spain	2 *0.19* (0.094)	2.30 *0.33* (0.142)	1.32 *0.06* (0.049)
Coir	*Cocos nucifera*	Sri Lanka	3 *0.31* (0.101)	4.17 *0.28* (0.068)	1.2 *0.08* (0.067)
Cotton	*Gossypium*	India	3 *0.19* (0.061)	2.50 *0.16* (0.062)	1.55 *0.05* (0.032)

Table 2. *Cont.*

Fibers	Plants	Origin	Diameter (mm)	Weight (g/m)	Density (g/cm^3)
Henequen	*Agave fourcroydes*	Mexico	2 *0.24* (0.121)	1.38 *0.33* (0.237)	1.45 *0.11* (0.079)
Jute	*Corchorus capsularis*	Bangladesh	3 *0.29* (0.099)	1.67 *0.16* (0.098)	1.37 *0.04* (0.029)
Flax	*Linum usitatissimum*	Netherlands	2 *0.34* (0.166)	0.76 *0.08* (0.101)	1.44 *0.07* (0.049)
Ramie	*Girardina diversifolia*	Nepal	1 *0.33* (0.330)	0.49 *0.08* (0.165)	1.35 *0.04* (0.031)
Raffia	*Raphia farinifera*	Madagascar	2.5 *0.19* (0.077)	0.60 *0.09* (0.146)	0.75 *0.02* (0.026)
Sisal	*Agave sisalana*	Brazil	2.5 *0.40* (0.159)	2.67 *0.06* (0.023)	1.45 *0.04* (0.027)

2.1. Hornification Process

Hornification is an environmentally friendly treatment that uses natural materials and does not produce waste. It consists of a series of wetting and drying cycles carried out until the fibers reach full saturation [28]. This process reduces the sensitivity of natural textiles to moisture while increasing their mechanical performance by promoting interfacial bonding.

The hornification process was performed at the Laboratory of Materials and Structures of the University of Florence (Italy). Water absorption tests were conducted to determine, for each type of fiber, the time required for complete saturation. All tests were performed at room temperature (18 °C; 53% humidity), without any preliminary drying treatment of the fibers. Each fiber specimen was 50 × 50 mm^2 and consisted of 5 warp and weft multifilaments. After measuring the initial dry weight ($W_{dry}{}^{0}$), the specimens were immersed in containers filled with water and weighed at regular intervals of 15 and 30 min. The testing process continued for a total of 180 min ($W_{wet}{}^{180}$), during which the specimen weight was monitored to identify the point of maximum saturation ($W_{wet}{}^{max}$), i.e., when no further weight increase was observed [49].

The maximum absorption capacity (WA) of each fiber was calculated using the following equation:

$$WA = \frac{W_{wet} - W_{dry}}{W_{dry}} \cdot 100(\%) \quad (2)$$

where W_{dry} is the initial weight of the dry specimen, and W_{wet} is the weight of the wet specimen.

After evaluating the absorption capacity (Figure 2a) of each type of fiber (Table 3), the specimens were immersed in water at room temperature (20 °C) until maximum saturation ($W_{wet}{}^{max}$) was reached (range 15–90 min) (Figure 2b). The next controlled drying phase was carried out using an oven equipped with electronic temperature control, set to reach and maintain a constant temperature of 50 °C [34].

Drying times ranged from 10 to 16 h [28], depending on the cellular structure of the fibers. After drying, the oven was set to gradually cool down to room temperature (20 °C) in order to avoid thermal shock. Five wet–dry cycles were conducted for each type of fiber. After each cycle, direct tensile tests were performed to evaluate the effects of the treatment on the mechanical properties of the fibers.

Finally, both treated and untreated fiber specimens were observed using a Gaia III (Tescan s.r.o, Brno, Czech Republic) FIB-SEM (Focused Ion Beam-Scanning Electron Microscope) to detect any structural changes induced by the hornification process.

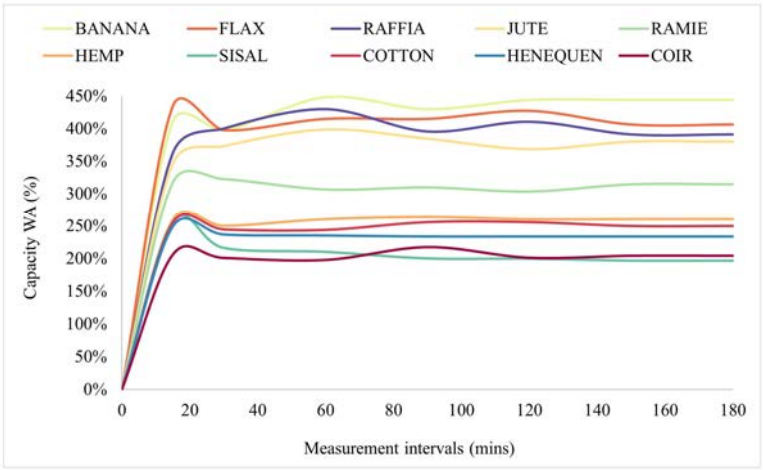

(a)

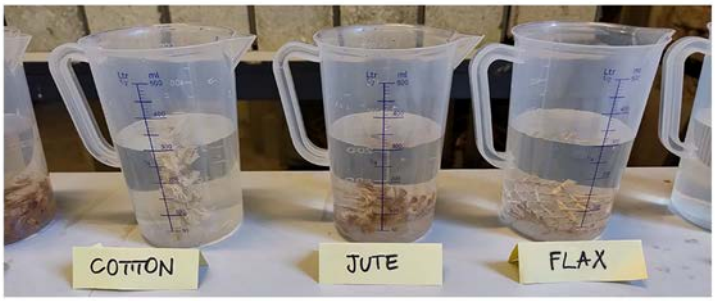

(b)

Figure 2. Absorption capacity of natural fibers: (**a**) absorption curves; (**b**) absorption tests.

Table 3. Results of the absorption tests.

Fibers	W_{dry}^{0} [g]	W_{wet}^{max} [g]	W_{wet}^{180} [g]	Maximum Absorption Time [min]	Absorption Capacity WA [%]
Banana	0.64	3.51	3.48	60	448
Hemp	1.77	6.43	6.37	90	263
Coir	4.23	13.41	12.85	90	217
Cotton	2.51	8.92	8.77	90	255
Henequen	1.92	6.7	6.4	15	249
Jute	2.18	10.87	10.46	60	399
Flax	0.81	4.33	4.1	15	435
Ramiè	0.63	2.66	2.61	30	322
Raffia	0.67	3.55	3.29	60	430
Sisal	3.29	11.7	9.75	15	256

2.2. Tensile Tests

Tensile tests were performed on natural fibers composed of 7 fiber bundles. Each specimen was 500 mm long and 65 mm wide. According to ACI 549.6R-20 [50], aluminum tabs—0.8 mm in thickness—were applied at both ends of the specimens. These tabs ensured a uniform distribution of tensile forces across all multifilaments during testing (Figure 3).

For each type of natural fiber, six tensile tests were carried out both before and after the hornification treatment. The tests were performed under displacement control at a rate of 0.4 mm/min using an Instron SATEC™ 5592-315HVL (Illinois Tool Works Inc., Glenview, IL, USA) universal testing machine, referenced in [16]. To accurately measure local displacements, a 50 mm strain gauge was applied in the middle of each specimen. Young's modulus was determined on the stress–strain curve as the slope of the linear elastic

branch and, in particular, it was determined between two points corresponding to 10% and 60% of the maximum tensile strength. The equivalent cross-sectional area of fiber textile was calculated according to CNR-DT 200 R1/2013 (2) [51]:

$$A_f = n \cdot w \cdot t_f \tag{3}$$

where A_f is the total resistant area expressed in mm^2, n is the number of bundles, w is the gap between bundles expressed in mm, and t_f is the equivalent thickness of a reinforcement mesh in the warp direction, and it was calculated according to CNR-DT 215/2018 [52]:

$$t_f = 1000 \cdot G/g \tag{4}$$

where G is the weight of the multifilaments in the warp direction expressed in daN/m^2, and g is the density of the fiber expressed in daN/m^3.

The weight (G) can be calculated as follows:

$$G = 1/1000 \cdot T_x/1000 \cdot N_f \tag{5}$$

where T_x is the linear density of the multifilament expressed in Tex [g/km], and N_f is the density of the fabric. The linear density of the multifilament, in accordance with EN ISO 1889:2009 [53], was calculated as follows:

$$T_x = P/L \cdot 1000 \tag{6}$$

where P is the weight of the multifilament expressed in g, and L is the length of the multifilament expressed in m.

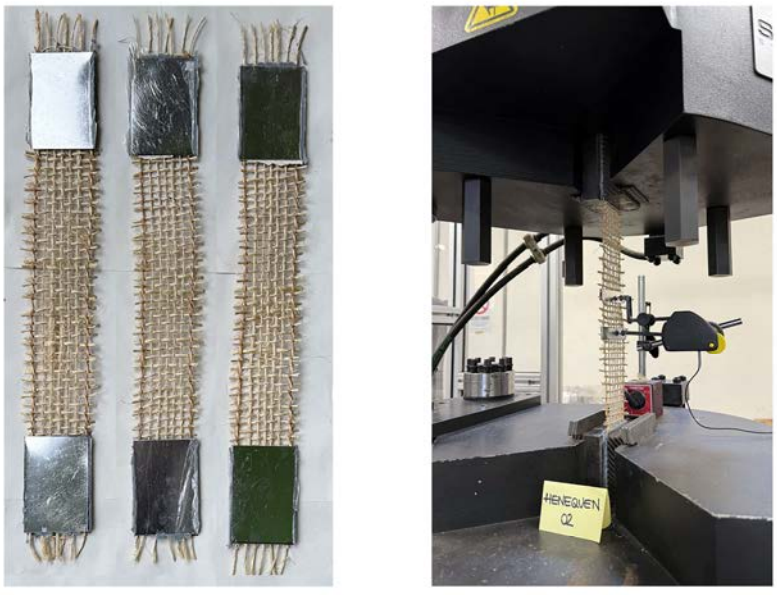

Figure 3. Tensile test results on henequen textile: (**a**) specimens; (**b**) tensile test setup.

3. Results

In Table 4, the results of direct tensile tests performed on untreated fiber textiles (N.H.: No Hornification) are summarized. The corresponding stress–strain curves are shown in Figure 4.

As can be observed, the values of the coefficient of variation (CV) range from 0.02 to 0.12. In virtue of this limited variability, the results can be considered reliable. In particular,

henequen (CV = 0.02) and jute (CV = 0.06) fibers exhibited highly homogeneous behavior, whereas flax (0.11) and banana (0.12) fibers showed a larger dispersion, probably due to morphological heterogeneity or practical issues in the specimen preparation. Overall, it can be confirmed that the data obtained from the tests on untreated specimens are reliable and representative of the average mechanical properties of the tested fibers.

Table 4. Tensile test results of natural textile (F_{max}: maximum load; σ_t: tensile stress; ε_u: ultimate strain; E: Young's modulus). The value of the standard variation is in italics, and the coefficient of variation is in parenthesis.

Fibers	Cycles	Af	F_{max} (N)	σ_t (MPa)	ε_u	E (GPa)
Banana	N.H.	6.88	436 *50.22* (0.12)	63 *7.30* (0.12)	0.027	3.01
Hemp	N.H.	12.13	2079 *164.42* (0.08)	171 *13.55* (0.08)	0.035	6.48
Coir	N.H.	24.17	1866 *184.41* (0.10)	77 *7.63* (0.10)	0.158	0.78
Cotton	N.H.	11.23	1146 *77.83* (0.07)	102 *6.93* (0.07)	0.142	0.76
Henequen	N.H.	6.65	905 *15.15* (0.02)	136 *2.28* (0.02)	0.028	7.73
Jute	N.H.	8.47	1704 *103.36* (0.06)	201 *12.20* (0.06)	0.025	10.23
Flax	N.H.	3.88	886 *97.94* (0.11)	228 *25.24* (0.11)	0.022	13.24
Ramiè	N.H.	5.02	769 *59.71* (0.08)	153 *11.89* (0.08)	0.021	7.25
Raffia	N.H.	5.57	230 *18.85* (0.08)	41 *3.38* (0.08)	0.059	0.67
Sisal	N.H.	12.82	2515 *238.42* (0.09)	196 *18.60* (0.09)	0.035	6.31

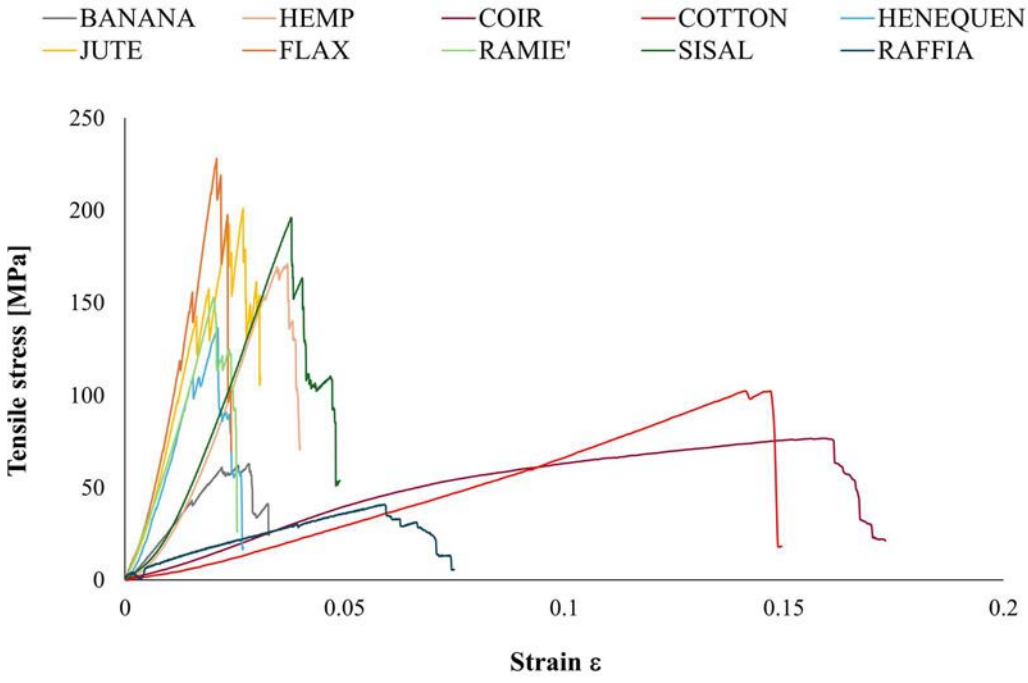

Figure 4. Tensile behavior of natural fibers: stress–strain diagrams.

The stress–strain diagrams showed for all specimens qualitatively similar behaviors. In particular, an initial pseudo-linear elastic branch was observed up to the maximum stress, followed by the failure of the external filaments of the specimen. Among the tested fibers, linen, sisal, and jute exhibited the highest tensile strength values. Conversely, raffia, coconut, and cotton highlighted considerably higher deformability when compared to the other types of fiber. At this first step of investigation, no clear correlations between water absorption and tensile properties were detected. Tensile tests were repeated after each hornification cycle, and the corresponding results are summarized in Table 5.

The values of the coefficients of variation reported in Table 5 are generally between 0.04 and 0.11, with an average value of basically below 10%. These results can be considered consistent with the tolerances commonly accepted for mechanical tests on natural fibers and composite material specimens. In particular, the lowest CV values (≈0.04–0.06)—observed in some tests—suggest the high stability of the mechanical behavior and a proper experimental test setup and execution. The slightly higher values (up to ≈0.11) observed in some tests (sisal, raffia, flax, and coir fibers) remained within acceptable limits, and this can be attributed to local differences in the fiber morphology or small irregularities during specimen preparation.

Table 5. Results of tensile tests on natural fibers after hornification (F_{max}: maximum load; σ_t: tensile stress; ε_u: ultimate strain; E: Young's modulus). The value of the standard variation is in italics, and the coefficient of variation is in parenthesis.

Fibers	Cycles	F_{max} (N)	σ_t (MPa)	ε_u	E (GPa)
Banana	H.I	467 *28.05* (0.06)	68 *7.75* (0.06)	0.030	2.43
	H.II	568 *25.00* (0.04)	83 *22.93* (0.04)	0.042	2.77
	H.III	617 *31.05* (0.05)	90 *24.86* (0.05)	0.040	2.34
	H.IV	707 *33.60* (0.05)	103 *9.28* (0.05)	0.039	3.02
	H.V	363 *22.61* (0.06)	53 *2.34* (0.06)	0.067	1.06
Hemp	H.I	1266 *51.68* (0.04)	104 *4.25* (0.04)	0.038	3.49
	H.II	1216 *109.34* (0.09)	100 *8.98* (0.09)	0.059	3.06
	H.III	1551 *133.84* (0.09)	128 *11.00* (0.09)	0.050	2.21
	H.IV	1366 *134.27* (0.10)	113 *11.03* (0.10)	0.053	3.22
	H.V	1227 *94.69* (0.08)	101 *7.78* (0.08)	0.080	2.42
Coir	H.I	1783 *153.19* (0.09)	74 *6.35* (0.09)	0.197	0.67
	H.II	1874 *202.26* (0.11)	78 *8.39* (0.11)	0.162	0.75
	H.III	1682 *161.45* (0.10)	70 *6.70* (0.10)	0.185	0.67
	H.IV	1450 *147.50* (0.10)	60 *6.12* (0.10)	0.196	0.50
	H.V	1774 *192.92* (0.11)	73 *8.00* (0.11)	0.167	0.68

Table 5. *Cont.*

Fibers	Cycles	F_{max} (N)	σ_t (MPa)	ε_u	E (GPa)
Cotton	H.I	936 *74.05* (0.08)	83 *6.56* (0.08)	0.173	0.67
	H.II	414 *31.05* (0.07)	37 *2.75* (0.07)	0.180	0.39
	H.III	880 *75.02* (0.09)	78 *6.65* (0.09)	0.142	0.67
	H.IV	799 *79.47* (0.10)	71 *7.05* (0.10)	0.152	0.58
	H.V	1104 *111.22* (0.10)	98 *9.86* (0.10)	0.143	0.75
Henequen	H.I	1496 *131.83* (0.09)	225 *19.82* (0.09)	0.034	11.10
	H.II	1849 *111.80* (0.06)	278 *16.81* (0.06)	0.028	11.82
	H.III	2128 *130.37* (0.07)	320 *19.60* (0.07)	0.032	11.76
	H.IV	1204 *68.25* (0.06)	181 *10.26* (0.06)	0.027	7.44
	H.V	1543 *67.27* (0.04)	232 *10.12* (0.04)	0.029	7.58
Jute	H.I	659 *64.21* (0.10)	78 *7.60* (0.10)	0.044	2.98
	H.II	549 *54.84* (0.10)	65 *6.49* (0.10)	0.045	1.89
	H.III	726 *57.30* (0.08)	86 *6.78* (0.08)	0.031	2.55
	H.IV	1134 *98.15* (0.09)	134 *11.62* (0.09)	0.043	3.56
	H.V	979 *89.82* (0.09)	116 *10.63* (0.09)	0.042	3.33
Flax	H.I	555 *47.26* (0.09)	143 *12.21* (0.09)	0.019	6.92
	H.II	334 *36.54* (0.11)	86 *9.42* (0.11)	0.015	6.02
	H.III	524 *43.09* (0.08)	135 *11.11* (0.08)	0.019	9.61
	H.IV	493 *23.39* (0.05)	127 *6.03* (0.05)	0.015	11.55
	H.V	376 *16.15* (0.04)	97 *4.16* (0.04)	0.018	8.03
Ramiè	H.I	474 *41.24* (0.09)	94 *8.18* (0.09)	0.043	2.22
	H.II	502 *39.59* (0.08)	100 *7.86* (0.08)	0.052	2.59
	H.III	420 *37.03* (0.09)	84 *7.35* (0.09)	0.054	2.65
	H.IV	494 *44.91* (0.09)	98 *8.91* (0.09)	0.060	4.56
	H.V	482 *46.89* (0.10)	96 *9.30* (0.10)	0.082	3.25

Table 5. *Cont.*

Fibers	Cycles	F_{max} (N)	σ_t (MPa)	ε_u	E (GPa)
Raffia	H.I	230 *20.30* (0.09)	41 *3.62* (0.09)	0.045	0.99
	H.II	234 *20.30* (0.11)	42 *3.62* (0.11)	0.056	0.89
	H.III	247 *21.63* (0.09)	44 *3.86* (0.09)	0.052	0.82
	H.IV	252 *23.00* (0.09)	45 *4.10* (0.09)	0.062	0.77
	H.V	201 *19.29* (0.10)	36 *3.44* (0.10)	0.083	0.67
Sisal	H.I	2641 *108.28* (0.04)	206 *8.45* (0.04)	0.039	6.84
	H.II	2500 *274.16* (0.11)	195 *21.39* (0.11)	0.041	6.94
	H.III	2064 *148.22* (0.07)	161 *11.56* (0.07)	0.031	4.69
	H.IV	2333 *119.35* (0.05)	182 *9.31* (0.05)	0.034	6.85
	H.V	2244 *109.28* (0.05)	175 *8.52* (0.05)	0.034	9.57

To evaluate the effect of the treatment cycles on the tensile performances of the ten tested fibers, a one-way analysis of variance (ANOVA) was conducted, and the resulting F-statistic (Fisher's test statistic) and *p*-value (probability value) determined whether differences were statistically significant ($p < 0.05$).

Then, a two-way analysis of variance (ANOVA) was carried out to evaluate the influence of the type of fiber, the number of hornification cycles, and their relationship with the tensile strength of the treated fibers. In Table 6, the results are reported.

Table 6. Two-way ANOVA results for effects of fiber type and hornification cycles on tensile strength (SS: sum of squares; df: degrees of freedom; MS: mean square; F: Fisher's test statistic; *p*: probability value; VE: variance explained).

	SS	df	MS	F	*p*	VE (%)
Fibers	1.03×10^6	9	114,029	981.6	<0.001	72
Cycles	39,855	5	7991	68.8	<0.001	3
Fibers × Cycles	319,924	45	7109	61.2	<0.001	23
Residuals	34,850	300	116			2

The statistical analysis revealed that all the factors considered significantly affected the mechanical response of the fibers ($p < 0.001$). The type of fiber was the dominant factor, accounting for the largest portion of the total variability (72%).

The number of hornification cycles also showed a certain effect (3% of the total variance), confirming that repeated drying–wetting treatments can modify the fiber performance, particularly during the first cycles. The significant interaction between the two factors (23% of the variance) demonstrated that the effect of hornification depends on the type of fiber, as already discussed. The residual variance (2%) represents the experimental error.

4. Discussion

The histogram in Figure 5 shows, at each hornification cycle (from H.I to H.V), the variation in the tensile strength of the ten types of fibers with respect to those in the untreated state. Both the benefits and limitations of the hornification process are clearly highlighted.

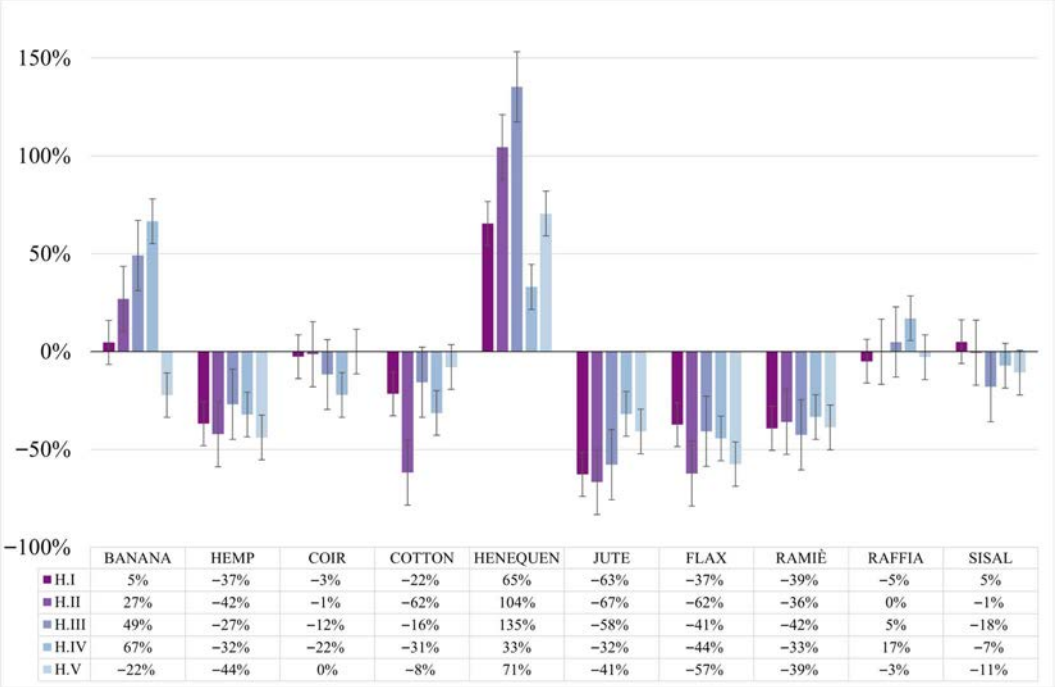

	BANANA	HEMP	COIR	COTTON	HENEQUEN	JUTE	FLAX	RAMIÈ	RAFFIA	SISAL
H.I	5%	−37%	−3%	−22%	65%	−63%	−37%	−39%	−5%	5%
H.II	27%	−42%	−1%	−62%	104%	−67%	−62%	−36%	0%	−1%
H.III	49%	−27%	−12%	−16%	135%	−58%	−41%	−42%	5%	−18%
H.IV	67%	−32%	−22%	−31%	33%	−32%	−44%	−33%	17%	−7%
H.V	−22%	−44%	0%	−8%	71%	−41%	−57%	−39%	−3%	−11%

Figure 5. Variation in tensile strength of fibers after hornification treatment.

The most notable variation in strength after the hornification treatment was observed in the henequen, sisal, and flax fibers.

In particular, the henequen fiber showed a significant increase (+65%) in tensile strength after the first cycle of treatment, while the highest increase (+135%) was observed after the third cycle. Sisal fiber exhibited a consistent trend through different hornification cycles, indicating good mechanical stability. An increase in strength (+5%) was observed after the first cycle, while a slight reduction was noted after the third (−18%), fourth (−7%), and fifth (−11%) cycles. Instead, the flax fiber showed an undesirable strong reduction in tensile strength after treatment. In particular, a reduction of 62% was observed after the second cycle, and a final reduction of 57% was observed after the five-cycle treatment.

The banana fiber exhibited a favorable trend, with a tensile strength which gradually increased up to 67% in the fourth cycle. However, this trend reversed in the fifth cycle, in which the strength was strongly reduced (−22%), probably due to a degradation of the structure of the internal fiber. This behavior confirmed the existence of an optimal threshold, beyond which the mechanical performance can reduce due to fatigue or damage to the internal structure of the fibers. The fibers of jute and flax showed a pronounced and consistent decrease in tensile strength after treatment. The jute fiber showed a strong decrease (−67%) after the second cycle, while the strength of the flax fiber steadily decreased (−57%) after the fifth cycle. These fibers highlighted a high vulnerability to the hornification process, probably due to a combination of high hydrophilicity, structural fragility, and micro-cracking induced by repeated humidity moisture fluctuations.

The cotton fibers showed a similar trend, with strength values that showed a reduction of 31% after the fourth cycle, although the recovery of strength after the fifth cycle suggests some reversible effects. Ramie fibers also showed a strength reduction (−42%) after the

third cycle. Hemp fibers highlighted negative values in all cycles (e.g., −42% after the second cycle, and −44% after the fifth cycle). Coir and sisal fibers showed relatively stable tensile strengths, with low variations after all cycles. In particular, for coir fibers, a strength variation between −3% (after the first cycle) and −12% (after the fourth cycle) was observed, while for sisal fibers, the variation was between +5% and −11%. Coir and sisal fibers slightly suffered swelling and internal rearrangements, probably thanks to their high lignin content and low water absorption.

The stress–strain curves of the henequen, sisal, and flax fibers are reported in Figure 6a–c, respectively. Different behaviors among the three types of textiles, after the hornification treatment, can be observed.

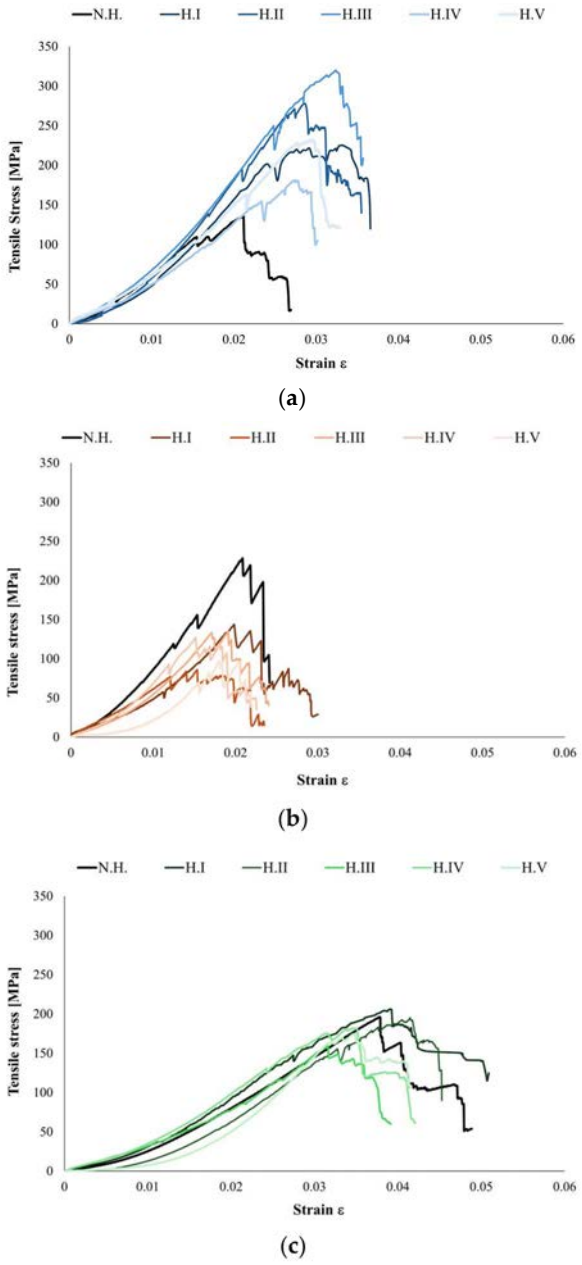

Figure 6. Tensile behaviors of fibers before and after hornification: (**a**) henequen, (**b**) flax, and (**c**) sisal.

The henequen textile showed a significant improvement in mechanical performance. In particular, the strength and stiffness increased up to the third cycle, probably due to effective microfibrillar reorganization and enhanced interfibrillar bonding. Flax fibers

exhibited a progressive and significant decrease in tensile strength and ultimate strain, probably indicating structural degradation due to their high hydrophilicity and low lignin content. In contrast, sisal fibers maintained an overall stable mechanical response, with limited variations in strength after the different cycles. This behavior confirms their good resilience and reduced sensitivity to the hornification process, probably due to their higher lignin content and lower water absorption capacity. Overall, the results confirm that the effectiveness of the hornification treatment is strongly fiber-dependent. Additional tests are necessary to more deeply evaluate the influence of hornification on the different types of fibers as a function of their composition.

The aforementioned results highlighted that hornification was the most effective on fibers with moderate to high initial water absorption capacities (e.g., banana, henequen), flexible microfibrillar structures, and a balanced ratio of cellulose to lignin. The exceptional performance of henequen fiber confirmed the strong synergy between the morphological characteristics of henequen and the rearrangement induced by hornification. The remarkable enhancement confirmed that repeated wet–dry cycles effectively improved the microfibrillar alignment and increased the stiffness by strengthening interfacial hydrogen bonds.

In contrast, brittle fibers underwent mechanical degradation due to fibril delamination, shrinkage-induced crack formation, or loss of interfibrillar cohesion.

In order to investigate the morphological changes after the hornification process, the fibers were qualitatively investigated using a Gaia III (Tescan s.r.o, Brno, Czech Republic) FIB-SEM (Focused Ion Beam-Scanning Electron Microscope). The electron beam used for SEM imaging had a voltage of 10 kV, operating in high-vacuum mode and with a secondary-electron (SE) detector. Samples were deposited on a stub and then coated with an ultrathin coating of silver.

By comparing the SEM images of untreated fibers to those subjected to hornification, clear morphological differences can be qualitatively observed.

Figure 7a–c illustrate the untreated state of the sisal fiber, and Figure 7d–f present some effects of hornification.

The treated fibers showed an increase in surface roughness and more pronounced longitudinal striations, which are associated with the alignment of cellulose microfibrils. However, the differences between treated and untreated sisal fibers are relatively subtle, as reflected in the tensile test results, which showed minimal variation. This suggests that sisal may require a greater number of hornification cycles to undergo substantial morphological and mechanical modifications, probably due to a lower sensitivity to moisture-induced changes.

In contrast, henequen fibers (Figure 8) exhibited a markedly different behavior. After treatment, a 140% increase in tensile strength was recorded, accompanied by evident morphological alterations.

SEM analysis revealed a cleaner fiber surface, free of superficial residues such as waxes, pectins, and soil particles. The surface is noticeably rougher, with enhancement in the adhesion property. The multifilament structure appears significantly more compact, with a reduction in lumen size. Unlike other natural fibers such as flax and jute, which showed progressive degradation, henequen maintained its structural integrity and mechanical performance, suggesting it as an optimal candidate for use in eco-sustainable composite materials.

In contrast, flax fibers (Figure 9) responded negatively to the hornification process, showing a 62% decrease in tensile strength after the second cycle of hornification.

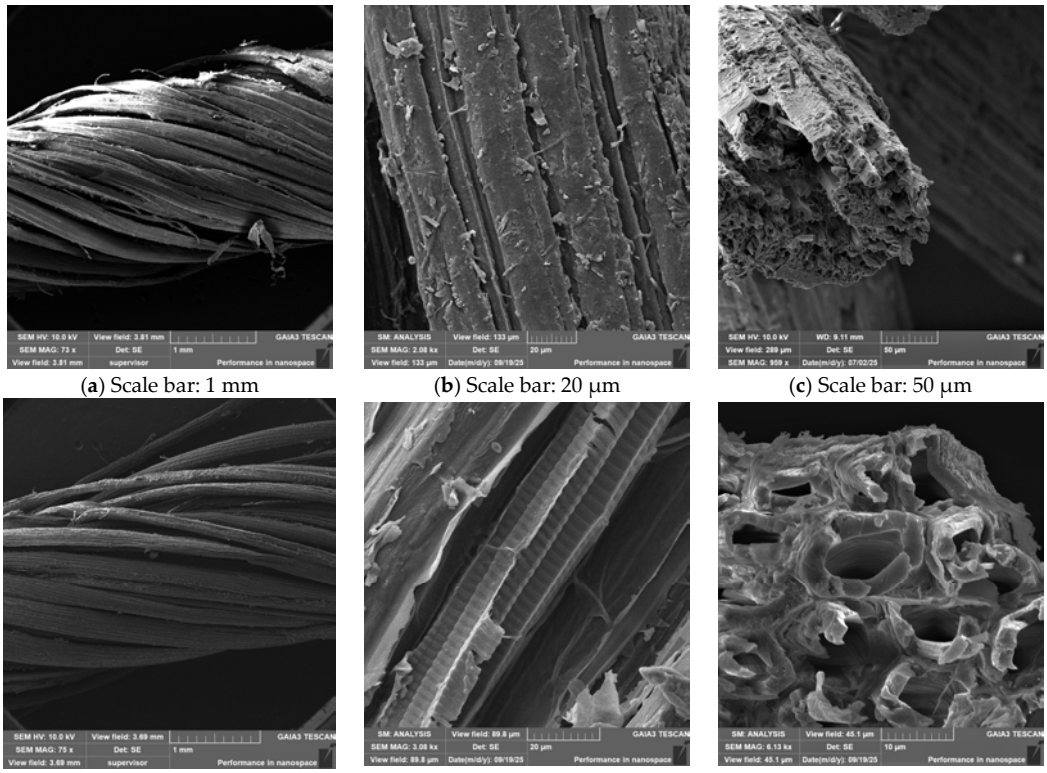

(**a**) Scale bar: 1 mm (**b**) Scale bar: 20 μm (**c**) Scale bar: 50 μm

(**d**) Scale bar: 1 mm (**e**) Scale bar: 20 μm (**f**) Scale bar: 10 μm

Figure 7. SEM image of sisal fibers: (**a**) multifilaments, N.H.; (**b**) fibrous bundle, N.H.; (**c**) cross section, N.H.; (**d**) multifilaments, H.III; (**e**) fibrous bundle, H.III; (**f**) cross section, H.III.

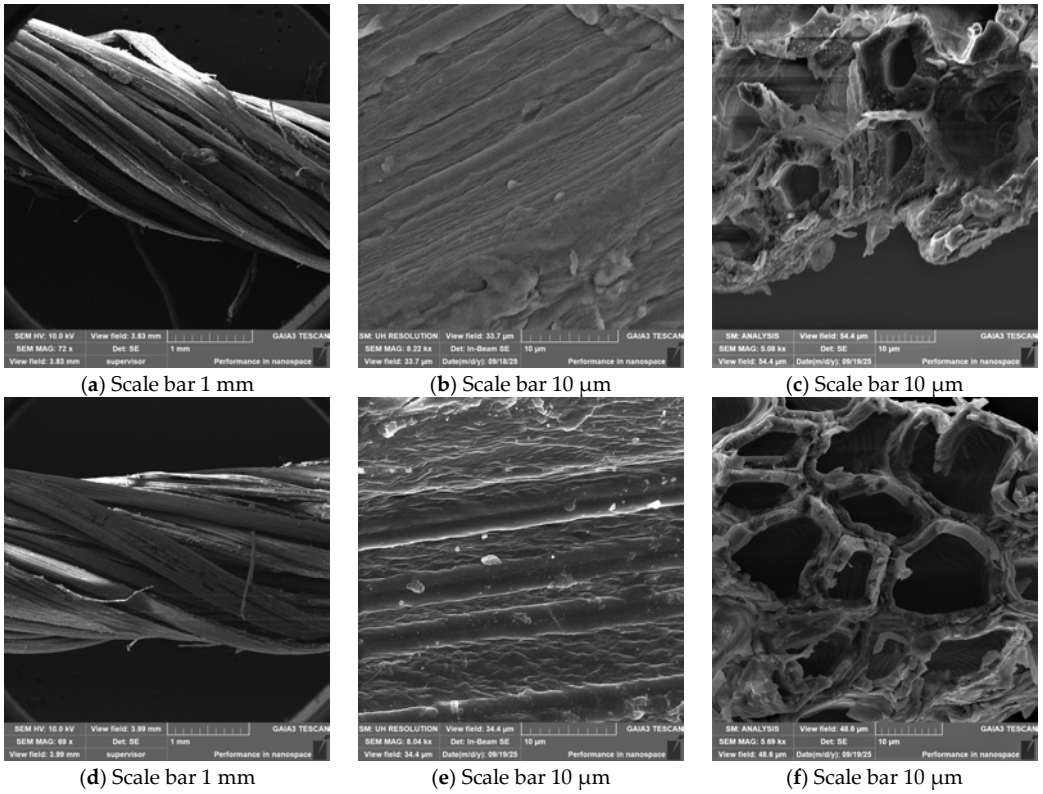

(**a**) Scale bar 1 mm (**b**) Scale bar 10 μm (**c**) Scale bar 10 μm

(**d**) Scale bar 1 mm (**e**) Scale bar 10 μm (**f**) Scale bar 10 μm

Figure 8. SEM images of henequen fibers: (**a**) multifilaments, N.H.; (**b**) fibrous bundle, N.H.; (**c**) cross section, N.H.; (**d**) multifilaments, H.III; (**e**) fibrous bundle, H.III; (**f**) cross section, H.III.

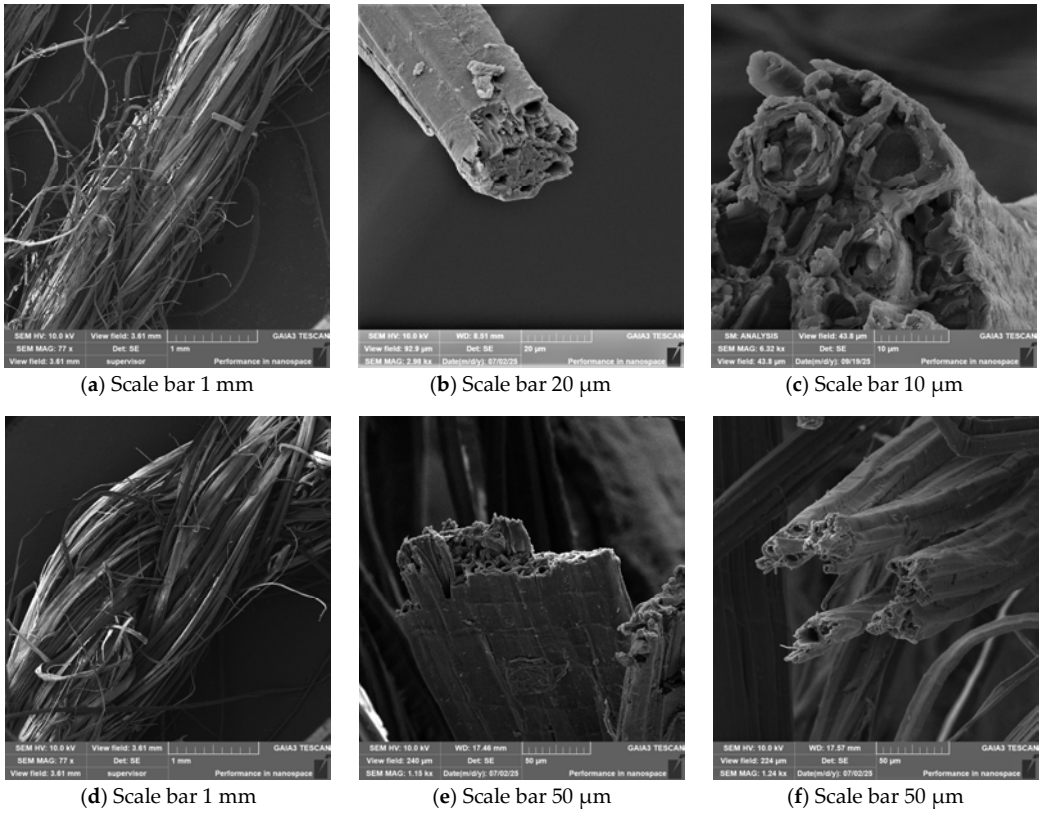

(**a**) Scale bar 1 mm (**b**) Scale bar 20 μm (**c**) Scale bar 10 μm

(**d**) Scale bar 1 mm (**e**) Scale bar 50 μm (**f**) Scale bar 50 μm

Figure 9. SEM images of flax fibers: (**a**) multifilaments, N.H.; (**b**) fibrous bundle, N.H.; (**c**) cross section, N.H.; (**d**) multifilaments, H.II; (**e**) fibrous bundle, H.II; (**f**) cross section, H.II.

SEM images revealed an excessive compaction of individual fibers and a collapse of the internal lumen, probably caused by mechanical fatigue induced by the repeated wetting and drying cycles. After moisture absorption, the cell wall tended to swell primarily in the transverse direction, but repeated cycles caused internal stress that progressively weakened the fiber's integrity.

In this context, the hornification process emerged as a promising and low-impact method to influence the mechanical properties of natural fibers, but optimization in terms of the number of cycles and fiber selection seems to be essential for more precise considerations and practical applications.

Furthermore, additional structural characterizations by XRD (X-Ray Diffraction) and FTIR (Fourier Transform Infrared Spectroscopy) devices are necessary in the future for an in-depth analysis of the different phenomena. X-ray photoelectron spectroscopy can be useful to accurately analyze the surface element composition (e.g., changes in the O/C ratio) of fibers before and after treatment, combining FTIR to evaluate the peak intensity changes of hydroxyl groups.

5. Conclusions

In this study, the mechanical performances of ten different natural fibers were investigated, with the aim of evaluating their suitability as sustainable reinforcement for innovative composite materials. The experimental campaign focused on tensile tests performed before and after a fully natural protective treatment known as the hornification process. In the context of an eco-friendly approach, no treatments with chemical agents were taken into account in this investigation.

In order to determine the effective number of hornification cycles for increasing the mechanical properties of the tested fibers, 30 tensile tests were performed on each type of fiber as the number of hornification cycles increased (from one to five).

In the untreated condition, fibers of hemp (171 MPa), jute (201 MPa), flax (228 MPa), and sisal (196 MPa) showed the highest tensile strength. After the hornification cycles (from one to five), the strength of banana had an increase of 58% (after four cycles), that of henequen had an increase of 140% (after three cycles), while the strengths of coir and sisal were slightly increased: 11% (after two cycles) and 8% (after one cycle), respectively. In contrast, jute and flax specimens showed high decreases in tensile strength after the hornification treatment. The jute fiber showed a decrease of 67% (after two cycles), and flax showed a decrease of 60% (after five cycles). All of the other fibers showed decreases in tensile strength, even if less pronounced with respect to jute and flax. These fibers, so vulnerable to the hornification process, are not truly suitable for embedment in any mortar matrix to constitute a green composite material.

The effects of the treatment on the morphological and mechanical properties of the fibers were qualitative analyzed by scanning electron microscopy (SEM).

After the hornification process, the morphological analysis showed that henequen and sisal benefited from increased compactness and fiber integrity, leading to enhanced mechanical properties.

These fibers appear to be promising candidates for use in eco-compatible composite materials for the strengthening of structural elements in contexts where environmental sustainability is a primary concern. Moreover, the use of a non-chemical treatment such as hornification preserves the biodegradability and renewability of the fibers, making the composite material both structurally effective and environmentally responsible. The results of this study represent a promising starting point: in the future, an extended experimental campaign and numerical simulations for optimizing multi-cycle hornification, checking the bond performances of composite materials assembled with natural fibers and their durability under real environmental conditions, are necessary to allow for more general considerations and practical recommendations.

Author Contributions: G.S., V.A., M.D.S., S.G., M.C.S. and M.L.S. contributed equally to this work. All authors have read and agreed to the published version of the manuscript.

Funding: This research received no external funding.

Data Availability Statement: The original contributions presented in this study are included in the article. Further inquiries can be directed to the corresponding authors.

Acknowledgments: This study was carried out within the RETURN Extended Partnership and received funding from the European Union Next-GenerationEU (National Recovery and Resilience Plan—NRRP, Mission 4, Component 2, Investment 1.3—D.D. 1243 2/8/2022, PE0000005). The financial support of the Italian Ministry of University and Research (MUR) through the PRIN2022 project 'Unified approach for improving structural and thermal response of masonry buildings with optimized sustainable composite materials—ASThRO-Co' is gratefully acknowledged.

Conflicts of Interest: The authors declare no conflicts of interest.

References

1. Naser, M.Z.; Hawileh, R.A.; Abdalla, J.A. Fiber-Reinforced Polymer Composites in Strengthening Reinforced Concrete Structures: A Critical Review. *Eng. Struct.* **2019**, *198*, 109542. [CrossRef]
2. Khodadadi, N.; Roghani, H.; Harati, E.; Mirdarsoltany, M.; De Caso, F.; Nanni, A. Fiber-Reinforced Polymer (FRP) in Concrete: A Comprehensive Survey. *Constr. Build. Mater.* **2024**, *432*, 136634. [CrossRef]
3. Minafò, G.; Cucchiara, C.; Monaco, A.; La Mendola, L. Effect of FRP Strengthening on the Flexural Behaviour of Calcarenite Masonry Walls. *Bull. Earthq. Eng.* **2017**, *15*, 3777–3795. [CrossRef]

4. Sandoli, A.; Ferracuti, B.; Calderoni, B. FRP-confined tuff masonry columns: Regular and irregular stone arrangement. *Compos. Part B Eng.* **2019**, *162*, 621–630. [CrossRef]
5. Alecci, V.; Galassi, S.; Mistretta, F.; Stipo, G.; De Stefano, M. Stability Assessment of Masonry Arches Reinforced with Fiber-Reinforced Composite Materials Under Large Deformation. *Lect. Notes Civ. Eng.* **2024**, *437*, 737–746. [CrossRef]
6. Di Tommaso, A.; Focacci, F.; Micelli, F. Strengthening Historical Masonry with FRP or FRCM: Trends in Design Approach. In *Key Engineering Materials*; Trans Tech Publications Ltd.: Zurich, Switzerland, 2017; Volume 747 KEM, pp. 166–173.
7. Bertolesi, E.; Torres, B.; Adam, J.M.; Calderón, P.A.; Moragues, J.J. Effectiveness of Textile Reinforced Mortar (TRM) Materials for the Repair of Full-Scale Timbrel Masonry Cross Vaults. *Eng. Struct.* **2020**, *220*, 110978. [CrossRef]
8. Kariou, F.; Triantafyllou, S.; Bournas, D. TRM strengthening of masonry arches: An experimental investigation on the effect of strengthening layout and textile fibre material. *Compos. Part B Eng.* **2019**, *173*, 106765. [CrossRef]
9. Zampieri, P.; Gonzalez-Libreros, J.; Simoncello, N.; Pellegrino, C. Strengthening of Masonry Arches with FRCM Composites: A Review. *Key Eng. Mater.* **2019**, *817*, 251–258. [CrossRef]
10. Alecci, V.; De Stefano, M.; Galassi, S.; Luciano, R.; Pugliese, D.; Stipo, G. Influence of Different Mortar Matrices on the Effectiveness of FRCM Composites for Confining Masonry Columns. *J. Test. Eval.* **2023**, *51*, 735–750. [CrossRef]
11. Alecci, V.; De Stefano, M.; Galassi, S.; Magos, R.; Stipo, G. Confinement of Masonry Columns with Natural Lime-Based Mortar Composite: An Experimental Investigation. *Sustainability* **2021**, *13*, 13742. [CrossRef]
12. Ferretti, F.; Khatiwada, S.; Incerti, A.; Giacomin, G.; Tomaro, F.; De Martino, V.; Mazzotti, C. Structural Strengthening of Masonry Elements by Reinforced Repointing Combined with FRCM and CRM. *Procedia Struct. Integr.* **2023**, *44*, 2254–2261. [CrossRef]
13. Alecci, V.; Fagone, M.; Galassi, S.; Rotunno, T.; Stipo, G.; De Stefano, M. Experimental Shear Behaviour of Masonry Walls Reinforced with FRCM. *Eng. Struct.* **2024**, *315*, 118425. [CrossRef]
14. Santandrea, M.; Daissè, G.; Mazzotti, C.; Carloni, C. An Investigation of the Debonding Mechanism between FRCM Composites and a Masonry Substrate. *Key Eng. Mater.* **2017**, *747*, 382–389. [CrossRef]
15. D'Antino, T.; Carloni, C.; Sneed, L.H.; Pellegrino, C. Matrix-Fiber Bond Behavior in PBO FRCM Composites: A Fracture Mechanics Approach. *Eng. Fract. Mech.* **2014**, *117*, 94–111. [CrossRef]
16. Dalalbashi, A.; Ghiassi, B.; Oliveira, D.; Freitas, A. Effect of test setup on the fiber-to-mortar pull-out response in TRM composites: Experimental and analytical modeling. *Compos. Part B* **2018**, *143*, 250–268. [CrossRef]
17. Calabrese, A.S.; D'Antino, T.; Colombi, P. Experimental and Analytical Investigation of PBO FRCM-Concrete Bond Behavior Using Direct and Indirect Shear Test Set-Ups. *Compos. Struct.* **2021**, *267*, 113672. [CrossRef]
18. De Santis, S.; Carozzi, F.; de Felice, G.; Poggi, C. Test methods for Textile Reinforced Mortar systems. *Compos. Part B* **2017**, *127*, 121–132. [CrossRef]
19. Kumar, S.; Manna, A.; Dang, R. A Review on Applications of Natural Fiber-Reinforced Composites (NFRCs). In *Materials Today: Proceedings*; Elsevier Ltd.: Amsterdam, The Netherlands, 2021; Volume 50, pp. 1632–1636.
20. Codispoti, R.; Oliveira, D.V.; Olivito, R.S.; Lourenço, P.B.; Fangueiro, R. Mechanical Performance of Natural Fiber-Reinforced Composites for the Strengthening of Masonry. *Compos. B Eng.* **2015**, *77*, 74–83. [CrossRef]
21. Mercedes, L.; Gil, L.; Bernat-Maso, E. Mechanical Performance of Vegetal Fabric Reinforced Cementitious Matrix (FRCM) Composites. *Constr. Build. Mater.* **2018**, *175*, 161–173. [CrossRef]
22. Asprone, D.; Durante, M.; Prota, A.; Manfredi, G. Potential of Structural Pozzolanic Matrix-Hemp Fiber Grid Composites. *Constr. Build. Mater.* **2011**, *25*, 2867–2874. [CrossRef]
23. Ferrara, G.; Pepe, M.; Martinelli, E.; Tolêdo Filho, R.D. Tensile Behavior of Flax Textile Reinforced Lime-Mortar: Influence of Reinforcement Amount and Textile Impregnation. *Cem. Concr. Compos.* **2021**, *119*, 103984. [CrossRef]
24. Fidelis, M.E.A.; Toledo Filho, R.D.; de Silva, F.A.; Mechtcherine, V.; Butler, M.; Hempel, S. The Effect of Accelerated Aging on the Interface of Jute Textile Reinforced Concrete. *Cem. Concr. Compos.* **2016**, *74*, 7–15. [CrossRef]
25. Lima, P.R.L.; Santos, M.; Camilloto, P.; Souza Cruz, R. Effect of Surface Biopolymeric Treatment on Sisal Fiber Properties and Fiber-Cement Bond. *J. Eng. Fibers Fabr.* **2017**, *12*, 155892501701200207. [CrossRef]
26. Abdollahiparsa, H.; Shahmirzaloo, A.; Teuffel, P.; Blok, R. A Review of Recent Developments in Structural Applications of Natural Fiber-Reinforced Composites (NFRCs). *Compos. Adv. Mater.* **2023**, *32*, 263498332211475. [CrossRef]
27. Laverde, V.; Marin, A.; Benjumea, J.M.; Rincón Ortiz, M. Use of Vegetable Fibers as Reinforcements in Cement-Matrix Composite Materials: A Review. *Constr. Build. Mater.* **2022**, *340*, 127729. [CrossRef]
28. Ferreira, S.R.; Silva, F.D.A.; Lima, P.R.L.; Toledo Filho, R.D. Effect of Fiber Treatments on the Sisal Fiber Properties and Fiber-Matrix Bond in Cement Based Systems. *Constr. Build. Mater.* **2015**, *101*, 730–740. [CrossRef]
29. Zugenmaier, P. Crystalline Cellulose and Derivatives: Characterization and Structures. In *Springer Series in Wood Science*; Springer: Berlin/Heidelberg, Germany, 2008.
30. Mai, Y.W.; Hakeem, M.I.; Cotterell, B. Effects of Water and Bleaching on the Mechanical Properties of Cellulose Fibre Cements. *J. Mater. Sci.* **1983**, *18*, 2156–2162. [CrossRef]

31. Coutts, R.S.P. Flax Fibres as a Reinforcement in Cement Mortars. *Int. J. Cem. Compos. Lightweight Concr.* **1983**, *5*, 257–262. [CrossRef]
32. Rocha Ferreira, S.; Rodrigues Sena Neto, A.; de Andrade Silva, F.; Gomes de Souza, F.; Dias Toledo Filho, R. The Influence of Carboxylated Styrene Butadiene Rubber Coating on the Mechanical Performance of Vegetable Fibers and on Their Interface with a Cement Matrix. *Constr. Build. Mater.* **2020**, *262*, 120770. [CrossRef]
33. Abbass, A.; Oliveira, D.V.; Lourenço, P.B.; Paiva, M.C. Multi-Scale Experimental Investigation on the Structural Behaviour of Novel Nanocomposite/Natural Textile-Reinforced Mortars. *Constr. Build. Mater.* **2024**, *444*, 137798. [CrossRef]
34. Abbass, A.; Paiva, M.C.; Oliveira, D.V.; Lourenço, P.B.; Fangueiro, R. Graphene/Polyurethane Nanocomposite Coatings—Enhancing the Mechanical Properties and Environmental Resistance of Natural Fibers for Masonry Retrofitting. *Compos. Part A Appl. Sci. Manuf.* **2023**, *166*, 107379. [CrossRef]
35. Menna, C.; Asprone, D.; Durante, M.; Zinno, A.; Balsamo, A.; Prota, A. Structural Behaviour of Masonry Panels Strengthened with an Innovative Hemp Fibre Composite Grid. *Constr. Build. Mater.* **2015**, *100*, 111–121. [CrossRef]
36. Singh, A.; Yadav, B.P. Sustainable Innovations and Future Prospects in Construction Material: A Review on Natural Fiber-Reinforced Cement Composites. *Environ. Sci. Pollut. Res.* **2024**, *31*, 62549–62587. [CrossRef] [PubMed]
37. Ferreira, S.R.; de Silva, F.A.; Lima, P.R.L.; Toledo Filho, R.D. Effect of Hornification on the Structure, Tensile Behavior and Fiber Matrix Bond of Sisal, Jute and Curauá Fiber Cement Based Composite Systems. *Constr. Build. Mater.* **2017**, *139*, 551–561. [CrossRef]
38. de Silva, F.A.; Chawla, N.; Filho, R.D. de T. Tensile Behavior of High Performance Natural (Sisal) Fibers. *Compos. Sci. Technol.* **2008**, *68*, 3438–3443. [CrossRef]
39. Charlet, K.; Baley, C.; Morvan, C.; Jernot, J.P.; Gomina, M.; Bréard, J. Characteristics of Hermès Flax Fibres as a Function of Their Location in the Stem and Properties of the Derived Unidirectional Composites. *Compos. Part A Appl. Sci. Manuf.* **2007**, *38*, 1912–1921. [CrossRef]
40. Baley, C. Analysis of the Flax Fibres Tensile Behaviour and Analysis of the Tensile Stiffness Increase. *Compos. Part A Appl. Sci. Manuf.* **2002**, *33*, 939–948. [CrossRef]
41. Kaith, B.S.; Mittal, H.; Jindal, R.; Maiti, M.; Kalia, S. Environment Benevolent Biodegradable Polymers: Synthesis, Biodegradability, and Applications. In *Cellulose Fibers: Bio- and Nano-Polymer Composites*; Springer: Berlin/Heidelberg, Germany, 2011; pp. 425–451.
42. Ren, G.; Yao, B.; Ren, M.; Gao, X. Utilization of Natural Sisal Fibers to Manufacture Eco-Friendly Ultra-High Performance Concrete with Low Autogenous Shrinkage. *J. Clean. Prod.* **2022**, *332*, 130105. [CrossRef]
43. Alves Fidelis, M.E.; Pereira, T.V.C.; Gomes, O.D.F.M.; De Andrade Silva, F.; Toledo Filho, R.D. The Effect of Fiber Morphology on the Tensile Strength of Natural Fibers. *J. Mater. Res. Technol.* **2013**, *2*, 149–157. [CrossRef]
44. Li, X.; Tabil, L.G.; Panigrahi, S. Chemical Treatments of Natural Fiber for Use in Natural Fiber-Reinforced Composites: A Review. *J. Polym. Environ.* **2007**, *15*, 25–33. [CrossRef]
45. Lakshmi Narayana, V.; Bhaskara Rao, L. A Brief Review on the Effect of Alkali Treatment on Mechanical Properties of Various Natural Fiber Reinforced Polymer Composites. *Mater. Today Proc.* **2021**, *44*, 1988–1994. [CrossRef]
46. Ali, A.; Shaker, K.; Nawab, Y.; Jabbar, M.; Hussain, T.; Militky, J.; Baheti, V. Hydrophobic Treatment of Natural Fibers and Their Composites—A Review. *J. Ind. Text.* **2018**, *47*, 2153–2183. [CrossRef]
47. Han, S.O.; Jung, Y.M. Characterization of Henequen Natural Fiber by Using Two-Dimensional Correlation Spectroscopy. *J. Mol. Struct.* **2008**, *883–884*, 142–148. [CrossRef]
48. Kharbanda, S.; Bhadury, T.; Gupta, G.; Fuloria, D.; Pati, P.R.; Mishra, V.K.; Sharma, A. Polymer Composites for Thermal Applications—A Review. *Mater. Today Proc.* **2021**, *47*, 2839–2845. [CrossRef]
49. Majumder, A.; Stochino, F.; Farina, I.; Valdes, M.; Fraternali, F.; Martinelli, E. Physical and Mechanical Characteristics of Raw Jute Fibers, Threads and Diatons. *Constr. Build. Mater.* **2022**, *326*, 126903. [CrossRef]
50. *ACI PRC-549.6R-20*; Guide to Design and Construction of Externally Bonded Fabric-Reinforced Cementitious Matrix (FRCM) and Steel-Reinforced Grout (SRG) Systems for Repair and Strengthening Masonry Structures. ACI Committee 549: Farmington Hills, MI, USA, 2020; ISBN 9781641951203.
51. *CNR-DT 200R1/2013*; Guide for the Design and Construction of Externally Bonded FRP Systems for Strengthening Existing Structures. National Research Council: Roma, Italy, 2013.
52. *CNR-DT 215/2018*; Guidelines for the Design and Execution of Strengthening of Existing Structures Using FRCM Systems. National Research Council: Roma, Italy, 2018.
53. *EN ISO 1889:2009*; Reinforcement Yarns—Determination of Linear Density. International Organization for Standardization (ISO): Geneva, Switzerland, 2009.